Production of simplex RNS and ROS by nanosecond pulse N_2/O_2 plasma jets with homogeneous shielding gas for inducing myeloma cell apoptosis

2017 J. Phys. D: Appl. Phys. 50 195204

(http://iopscience.iop.org/0022-3727/50/19/195204)

IOP Publishing Journal of Physics D: Applied Physics

J. Phys. D: Appl. Phys. **50** (2017) 195204 (9pp) https://doi.org/10.1088/1361-6463/aa66f0

Production of simplex RNS and ROS by nanosecond pulse N_2/O_2 plasma jets with homogeneous shielding gas for inducing myeloma cell apoptosis

Zhijie Liu[1], Dehui Xu[1], Dingxin Liu[1], Qingjie Cui[1], Haifeng Cai[1], Qiaosong Li[1], Hailan Chen[2,3] and Michael G Kong[1,2,3]

[1] State Key Laboratory of Electrical Insulation and Power Equipment, Centre for Plasma Biomedicine, Xi'an Jiaotong University, Xi'an City 710049, People's Republic of China
[2] Frank Reidy Center for Bioelectrics, Old Dominion University, Norfolk, VA 23508, United States of America
[3] Department of Electrical and Computer Engineering, Old Dominion University, Norfolk, VA 23529, United States of America

E-mail: dehuixu@hotmail.com (D Xu) and mglin5g@gmail.com (MGK)

Received 10 November 2016, revised 26 February 2017
Accepted for publication 15 March 2017
Published 18 April 2017

Abstract

In this paper, atmospheric pressure N_2/O_2 plasma jets with homogeneous shielding gas excited by nanosecond pulse are obtained to generate simplex reactive nitrogen species (RNS) and reactive oxygen species (ROS), respectively, for the purpose of studying the simplex RNS and ROS to induce the myeloma cell apoptosis with the same discharge power. The results reveal that the cell death rate by the N_2 plasma jet with N_2 shielding gas is about two times that of the O_2 plasma jet with O_2 shielding gas for the equivalent treatment time. By diagnosing the reactive species of $ONOO^-$, H_2O_2, OH and O_2^- in medium, our findings suggest the cell death rate after plasma jets treatment has a positive correlation with the concentration of $ONOO^-$. Therefore, the $ONOO^-$ in medium is thought to play an important role in the process of inducing myeloma cell apoptosis.

Keywords: nanosecond pulse, homogeneous shielding gas, reactive species, cell death rate, myeloma cell

(Some figures may appear in colour only in the online journal)

1. Introduction

In recent years, plasma–liquid interaction is a relatively new research field [1–3] and has gone through an explosion of attention in a range of biological and medical applications, such as disinfection, decontamination, wound healing and cancer therapy [4–8]. Generally, atmospheric pressure cold plasma jet (APPJ) interacting with a living cell is the presence of a gas–liquid environment, in which the APPJ typically occurs in humid air and is closer or even in contact with the gas–liquid interface [1–6]. As we know, various reactive oxygen and nitrogen species (RONS) can be produced by APPJ in the gas–liquid environment. Among the RONS, the OH, O, O_3, H_2O_2 as a main reactive oxygen species (ROS) and nitric oxide, NO_2^-, NO_3^- and peroxynitrites ($ONOO^-$) as a main reactive nitrogen species (RNS) are generally accepted to play a significant role in the inducing cell apoptosis process [9, 10]. The knowledge of ROS and RNS is mostly limited in the gas phase, not directly relevant to the targets to be treated in a humid environment or in a liquid phase [7, 11–14]. In

fact, various types of plasma-chemical reactions can be initiated and much of the primary and secondary RONS can be formed by APPJ at the gas–liquid interface, and then dissolve and diffuse into the liquid phase to initiate chemical and biocidal processes [14–16], which are not only dependent on the involved plasma jets source, but also on the composition of the exposed physiological liquids [17]. However, how gaseous reactive species may be correlated to liquid phase constituents is still unclear, as is the physico-chemical behavior of ROS and RNS in the liquid phase. More important is that the precise determination of the constituents and production of RONS in the liquid phase linked to inducing the apoptosis process is a critical bottleneck [7, 18]. Hence, the diagnosis of the production and control of the RONS in the liquid phase have become more and more important and valuable for further mechanism research of cancer cell apoptosis. Additionally, abundant research works have mainly focused on using He, Ar, N_2, ambient air or mixture gas as the working gas to produce APPJ, which have controlled the delivery of ROS and RNS into the liquid to induce cell apoptosis [4, 5, 8, 10, 13–21]. But most of the APPJ have in common that the major reactive species produced in the APPJ generate when the electrons and components of dissociated, excited and ionized gas interact with the surrounding air. Consequently, the composition of the RONS produced by the APPJ and the subsequent effects on cells can vary hugely, owing to the working gas and ambient conditions [17, 18]. In this paper, two kinds of working gas (N_2 and O_2) APPJs with homogeneous (N_2 and O_2) shielding gas are excited by a nanosecond pulse to generate simplex RNS and ROS, respectively, for the purpose of comparative study of the death rate for ROS and RNS inducing the myeloma cell apoptosis process.

2. Experimental methods

Figure 1(a) shows the schematic illustration of the experimental setup of the APPJ. The APPJ device consists of two tubes: One is the outer tube with a length of 10 cm, which is a transparent plastic tube with inner and outer diameters of 6 mm and 8 mm, respectively. The other tube is a quartz tube with a length of 6 cm and inner and outer diameters of 1 mm and 2 mm, respectively, inserted inside the plastic tube. A stainless steel needle with a diameter of about 0.1 mm is fixed in the center of the quartz tube as a high voltage electrode, and is 15 mm away from the nozzle of the quartz. A 10 mm long ring copper electrode wrapped around the quartz tube at a distance of 10 mm from the nozzle end serves as the grounded electrode. Pure N_2 or O_2 as the working gas are injected though inlet I into the quartz tube with a flow rate of 300 sccm; the homogenous gas (N_2 and O_2) as the shielding gas are flowed though inlet II into the plastic tube with a flow rate of 3 slm. The aim of the shielding gas is to isolate and shield ambient air, avoiding that which reacts with the components of APPJ to generate new RNS and ROS. A nanosecond pulse generator with a pulse rate of 4 kHz, a rising time of 40 ns and a pulse duration of 1 μs is used to generate APPJ. The waveforms of the pulse voltage and current are measured by a digital oscilloscope (Tektronix DPO3000) equipped with voltage/current probes (P6015A and P6021) and the optical emission spectroscopy (OES) of APPJ is detected by a monochromator (Andor SR-750i, grating grooving 1200 lines mm^{-1}). The fiber optic is oriented up the APPJ axis; the location of the optical fiber is not moving when the OES is measured in the experimental process.

The LP-1 multiple myeloma cell, which has been reported in a previous study [22], is utilized to induce death by APPJ treatment in this experiment. The myeloma cell in medium (rpmi1640 culture fluid) is refreshed 24 h before performing the experiment, and then 100 μl of the medium added in a 96-well plate is placed under the nozzle of the quartz tube; the depth of the medium in the well plate is around 3 mm, the distance from the nozzle to the surface of the medium is 15 mm. A blank well between the treated wells is to avoid the cross contamination of wells adjacent with the APPJ treatment. Each experiment's data is repeated three times and the results are presented as mean $\pm$ SD in the below figures. Four separate well plates are used for cell viability analysis by the APPJ operating with four different gas chemistries. A Cell titer-glo assay (Promega, Madison, WI, USA) is used to assess cell viability at 24 h and 48 h after 30 s, 60 s and 120 s. PI staining indicating the cell death is performed and analyzed by a flow cytometer. 24 h after treatment of APPJs, 2 μl PI (50 μg ml^{-1}) are added into the medium and incubated at room temperature in the dark for 15 min. Peroxynitrite ($ONOO^-$) is detected by a fluorescent probe called coumarin boronic acid (CBA) (Item No. 14 051, Cayman Chemical Company) [23, 24]. CBA is incubated with samples at 20 μM for 30 min and fluorescence is detected by a microplate reader at an excitation of 332 nm and an emission of 420 nm. The H_2O_2 concentration is measured by Amplex Red Hydrogen Peroxide Assay (Invitrogen). The short lifetime reactive species O_2^- and OH produced by APPJ can first react with radical trapping agents Tempone-H and DMPO in the medium to form a stable and long lived spin-trapped adduct and subsequently be detected with an electron spin resonance spectrometer (ESR) [2, 24, 25]. Tempone-H and DMPO are respectively added at a final concentration of 1 mM and 100 μM prior to APPJ treatment. A Sodium Peroxynitrite (ONOONa) (Item No. 81 565, Cayman Chemical Company) is used to verify the plotting cell viability as a function of the concentration of $ONOO^-$.

In order to have a more convenient and scientific comparison research of the death rate for ROS and RNS inducing the myeloma cell apoptosis, both the average discharge power of N_2/N_2 APPJ at 9.2 kV and O_2/O_2 APPJ at 10.2 kV are fixed at 0.2 W, and the corresponding waveforms of pulse voltage, discharge current and average power are shown in figure 1(b). The discharge current is obtained by subtracting the displacement current from the total current, and there is only one main discharge current peak in the rising period of the pulse voltage. During the pulse voltage falling processing, another small discharge current peak is also present due to the secondary electron emission effect generated by negative feedback of the pulse voltage [26, 27]. The average power is calculated by the method in [26]. Meanwhile, the images of four types of APPJ, including N_2 APPJ with a N_2 shielding gas (N_2/N_2), N_2 APPJ

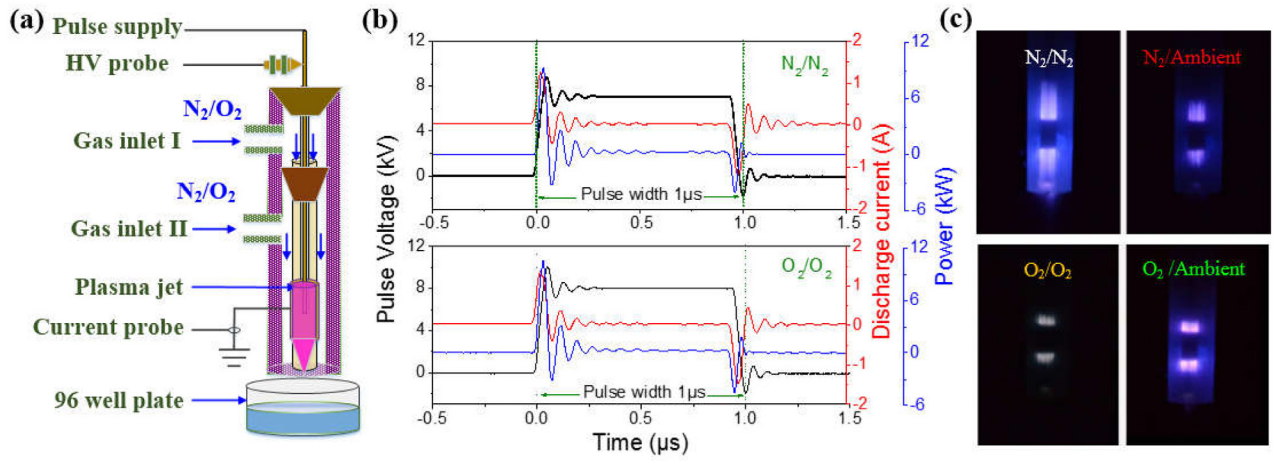

Figure 1. (a) Schematic illustration of the experimental setup of APPJ. (b) The waveforms of pulse voltage, discharge current, and average power of N_2/N_2 and O_2/O_2 APPJ, (c) the images of N_2/N_2, N_2/Ambient, O_2/O_2, and O_2/Ambient APPJ, respectively.

without a shielding gas (N_2/Ambient), O_2 APPJ with an O_2 shielding gas (O_2/O_2), and O_2 APPJ without a shielding gas (O_2/Ambient), are shown in figure 1(c) with the expose time for the former two types of 0.2 s and the expose time for the latter two types of 2 s. It is found that, for N_2/N_2 APPJ, the APPJ gets more intense by adding N_2 shielding gas, while for O_2/O_2 APPJ, the additional O_2 shielding gas can effectively avoid air composition to be involved in the discharge and the discharge color displays a bright white [28]. Without the O_2 shielding gas, the discharge intensity becomes stronger and the color presents pink. It can be seen that the APPJs plume actually exits the glass nozzle except for the O_2/O_2 APPJ, and the N_2/N_2 APPJs propagates the farthest and has a plume with a length of about 5 mm outside the quartz tube. However, it should be noted that the above mentioned APPJs could not touch the treated surface of medium, so the etching effect could be ignored in our experiment.

3. Experimental results

In order to identify the gaseous reactive species of four types APPJ in figure 1(c), the OES in the wavelength range from 300 to 800 nm is obtained in figures 2(a) and (b). As for the spectra of N_2/N_2 APPJ in figure 2(a), both of which mainly consist of N_2 ($C^3\Pi_u \rightarrow B^3\Pi_g$), N_2^+ ($B^2\sum_u^+ \rightarrow X^2\sum_g^+$), secondary diffraction of NO ($A^2\Sigma \rightarrow X^2\Pi$) and secondary diffraction of N_2 ($C^3\Pi_u \rightarrow B^3\Pi_g$). The N_2 ($C^3\Pi_u \rightarrow B^3\Pi_g$) is produced by electron impact excitation from the ground state N_2 ($X^2\sum_g^+$) and first metastable state N_2 ($A^2\sum_u^+$) [29]. The secondary diffraction of NO ($A^2\Sigma$) is relatively weaker and mainly produced by the reaction between N_2 ($A^2\sum_u^+$) and NO ($X^2\Pi$) due to the rapid energy transfer process [30]. The generation of the state N_2^+ ($B^2\sum_u^+$) is mainly though the direct electron collisions with high energy electrons [29]. Additionally, it is found that the emission intensity of N_2/N_2 APPJ is about two times higher compared to that of N_2/Ambient APPJ.

As for the spectra of O_2/O_2 APPJ in figure 2(b), a group of oxygen atomic lines for O ($3p^5P \rightarrow 3s^5S_2^o$) at 777.1 nm can be observed, which correspond to O(I) triplet state transitions; the generation of the state O ($3p^5P$) is ascribed to the direct electron-molecule dissociative collision molecule. More interesting is that only oxygen atomic O ($3p^5P \rightarrow 3s^5S_2^o$) lines can be observed in O_2/O_2 APPJ, so it is confirmed that the protective effect for the O_2 shielding gas is fully embodied and can effectively guarantee the air composition will not be involved in the discharge reaction process. As for O_2/Ambient APPJ, in addition to oxygen atomic O ($3p^5P$) lines, the N_2 ($C^3\Pi_u \rightarrow B^3\Pi_g$) and N_2^+ ($B^2\sum_u^+ \rightarrow X^2\sum_g^+$) can also be seen since the ambient air, especially N_2, participates in the reaction. These results are in good agreement with the literature published by Girard *et al* [18] who used O_2 as the shielding gas. According to the results in figures 2(a) and (b), it is found that the N_2/N_2 and O_2/O_2 APPJs can generate simplex RNS and ROS, respectively, some of which, such as NO and O, are considered to be the effective agents in inducing the cell death.

As for the difference in APPJ treatment with and without shielding gas, there is a lurking variable of flux to the cells, i.e. gas flow rate, when a shielding gas is present, the reactive species produced by APPJs would be carried along with the shielding gas to the liquid surface, but when the shielding gas is absent, the reactive species only diffuse slowly to the liquid surface, due to the low flow rate of 300 sccm. There are two types of ways for the reactive species to move toward the liquid surface [28]. However, in this paper, we mainly focus on the comparative study between N_2/N_2 APPJ treatment and O_2/O_2 APPJ treatment.

Next, we focus on the biological effects of simplex RNS and ROS produced by N_2/N_2 and O_2/O_2 APPJs on myeloma tumor cells. Figure 3(a) shows that cell viability is dramatically decreased 24 h after N_2/N_2 APPJ treatment for 30 s, while treatment by O_2/O_2 APPJ results in less cell death, compared to N_2/N_2 APPJ, indicating that RNS might be more dominant for myeloma cell apoptosis. The same tendency is found 48 h after treatment of N_2/N_2 and O_2/O_2 APPJ (figure 3(b)). According to our experience, if the cell viability is around 30–60% at post treatment 24 h, there may be a balance between the dying cells and the proliferating cells [31], therefore, in the following experiments, we only demonstrate the

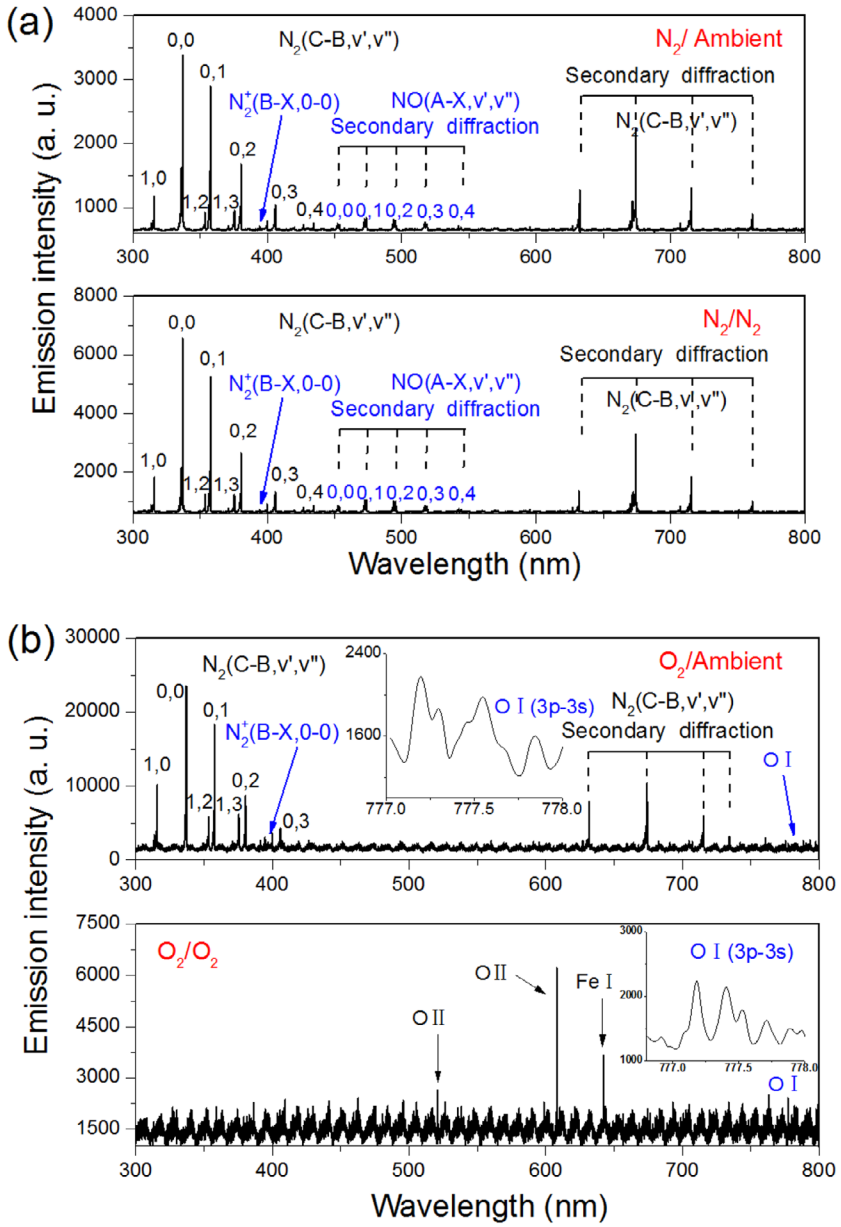

Figure 2. The OES produced by APPJ. (a) N_2/Ambient and N_2/N_2 APPJs, (b) O_2/Ambient and O_2/O_2 APPJs.

effects 24 h after plasma treatment, and the biological effects by four types APPJ (figure 1(c)) treatment are further compared. Figure 3(c) shows that N_2/Ambient APPJs induce more cell death than O_2/O_2 and O_2/Ambient APPJs under the same treatment time.

To further quantitatively analyze the cell death induced by N_2/N_2, N_2/Ambient, O_2/O_2 and O_2/Ambient APPJ, the percentage of dead cells (PI^+ cells) 24 h after APPJ treatment is calculated by flow cytometry in figure 4. It is revealed that gas control without APPJ treatment results in around 20% of cell death, due to the dry effect. Additionally, the results also reveal that the cell death rate by N_2 plasma jet, with or without N_2 shielding gas, is more than two times that of the O_2 plasma jet with or without O_2 shielding gas for the same treatment times, which is in good agreement with the result in figure 3. Meanwhile, the statistical results of the cell death calculated by flow cytometry are presented in figure 5, as for N_2/N_2 and O_2/O_2 APPJs treatment for 60 s, the cell death rate significantly increases up to approximately $91 \pm 5.6\%$ and $44 \pm 3.5\%$, respectively. The cell death rate moderately increases to $90\% \pm 3.8\%$ and $37 \pm 4.2\%$ after N_2/Ambient and O_2/Ambient APPJs treatment for 60 s. These results are in good agree,emt with that in figure 3, and reveal that the cell death rate of N_2/N_2 APPJ is about two times that of the O_2/O_2 APPJ for the equivalent treatment time. In this experiment, we use the microplate reader and the flow cytometry to detect cell death in figures 3 and 4, respectively, but it is found that the gas control in figure 4 causes 20% cell death, but not in figure 3. The reason may be explained as follows: in figure 3, the microplate reader would only detect the viable cell count, which, in the control group, is normalized as a criteria. In fact, the control group also presents a small amount of dead cells, due to the dry effect. Meanwhile, in figure 4, the flow cytometry would detect the proportion of living and dead cells at a

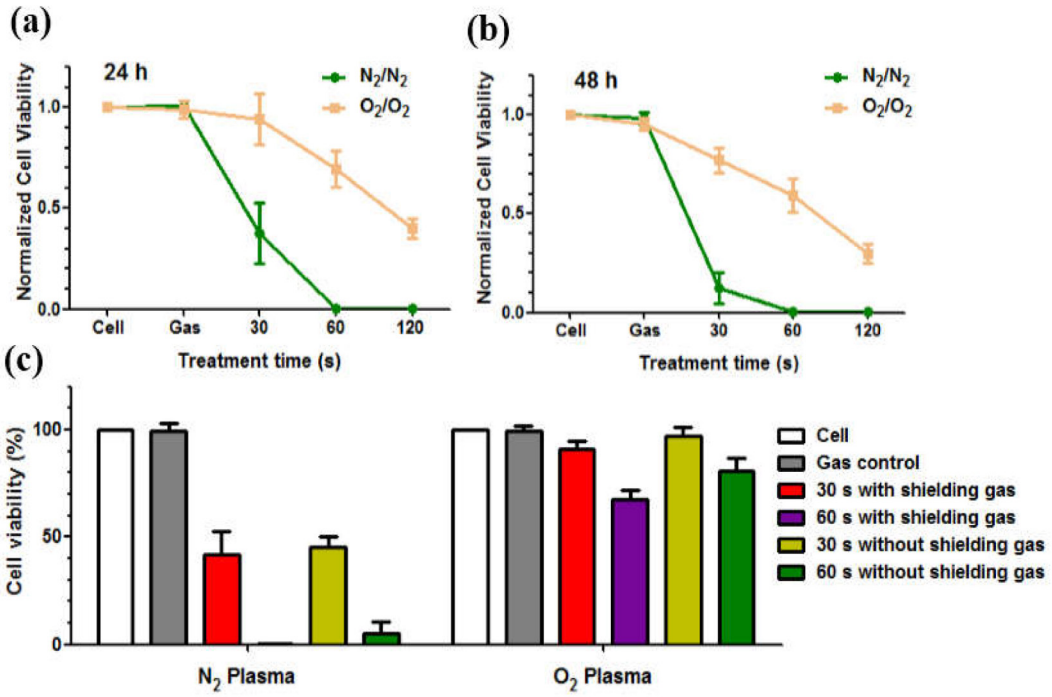

Figure 3. Cell viability analysis after N_2/N_2 and O_2/O_2 APPJs treatment for 24 h (a) and 48 h (b), respectively, (c) cell viability 24 h after treatment of N_2/N_2, N_2/Ambient, O_2/O_2, and O_2/Ambient APPJs.

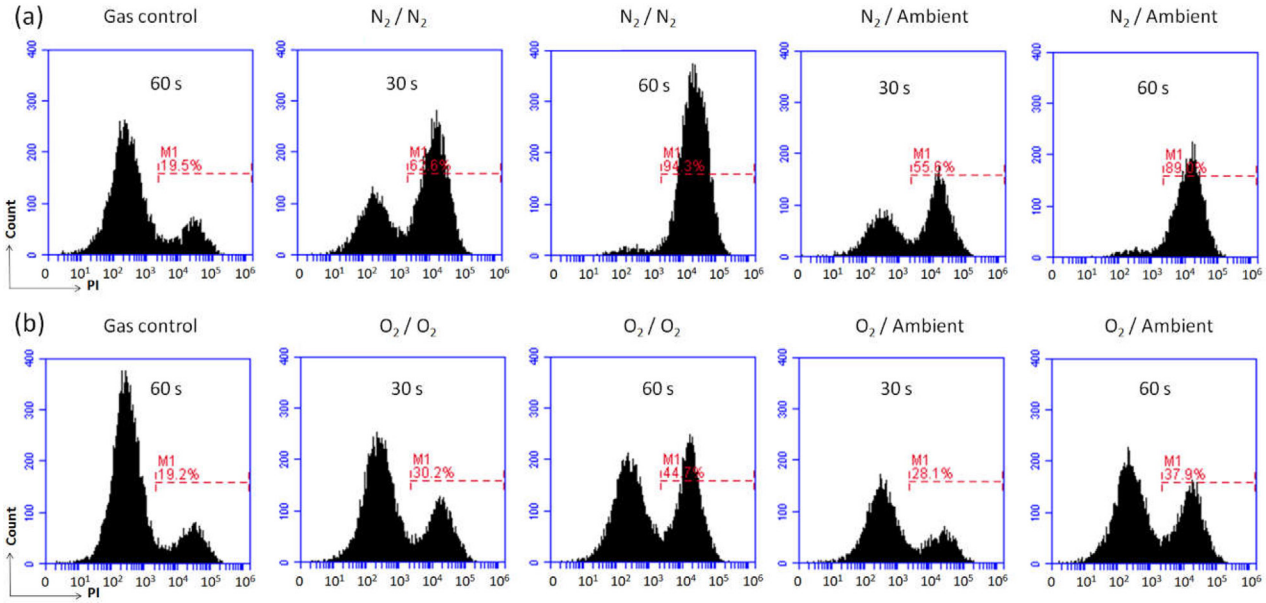

Figure 4. Percentage of dead cells (PI staining) analyzed by flow cytometer 24 h after N_2/N_2 and N_2/Ambient (a) and O_2/O_2 and O_2/Ambient (b) APPJs treatment.

time, about 80% living cells in figure 4 are actually equal to the 100% cell viability in the control group in figure 3.

To understand the different responses of myeloma cells to N_2/N_2, N_2/Ambient, O_2/O_2, and O_2/Ambient APPJs, the concentration of RNS and ROS in the medium after APPJ treatment is measured. Figure 6(a) shows that the concentration of $ONOO^-$ after N_2/N_2 and N_2/Ambient APPJs treatment is much more than that after O_2/O_2 and O_2/Ambient APPJs treatment. Additionally, the O_2/Ambient APPJ seems to produce a little more concentration of $ONOO^-$ compared to O_2/O_2 APPJ, which may be attributed to the ambient air involved in the discharge process. As shown in figure 6(b), the H_2O_2 concentration has no significant difference between the N_2 APPJ and O_2 APPJ with or without shielding gas, and almost keeps at the same level. Figure 6(c) shows that the concentration of O_2^- is relatively low after N_2 APPJ treatment, while O_2 APPJ treatment results in a higher O_2^- production. For OH, no OH signal is detected in N_2/N_2 APPJ treatment, while a clear OH signal could be detected in O_2/O_2 APPJ (figure 6(d)). Both of the characteristic signals of O_2^- and OH are inserted

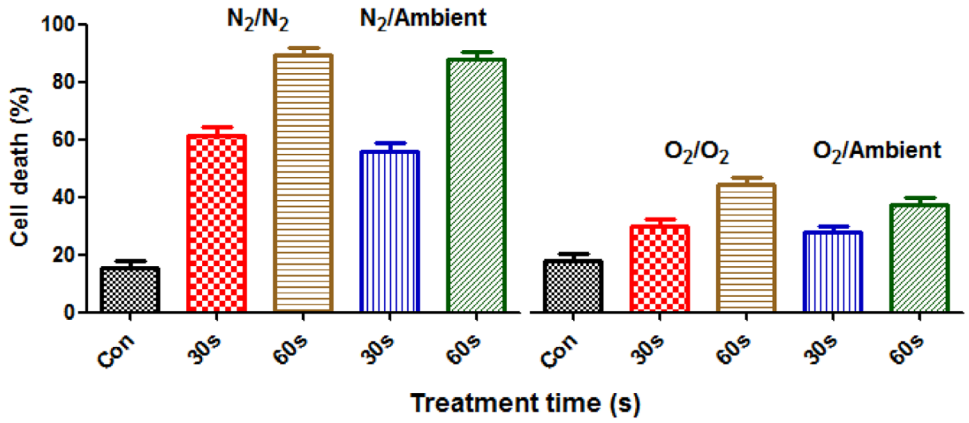

Figure 5. The statistical result of cell death measured by flow cytometry after treatment of N_2/N_2, N_2/Ambient, O_2/O_2, and O_2/Ambient APPJs treatment.

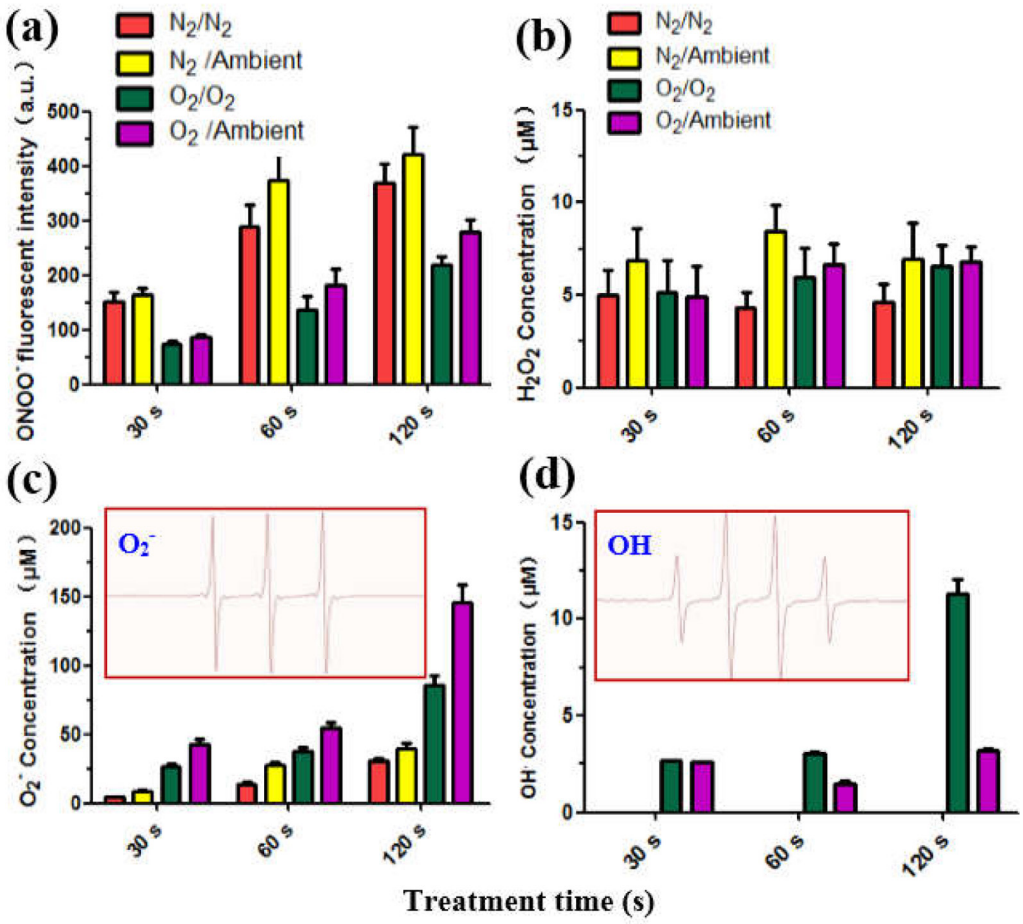

Figure 6. Reactive species $ONOO^-$ (a) and H_2O_2 (b) were measured by microreader after treatment of N_2/N_2, N_2/Ambient, O_2/O_2, and O_2/Ambient APPJs. Concentration of O_2^- (c) and OH (d) are detected by ESR after N_2/N_2, N_2/Ambient, O_2/O_2, and O_2/Ambient APPJs treatment.

in figures 6(c) and (d), respectively. Interestingly, the N_2/N_2 APPJ greatly decreases the production of OH, which indicates that the involvement of N_2 has a negative correlation to OH production.

In order to directly confirm that the $ONOO^-$ would effectively induce the LP-1 myeloma cell inactivation, a scatter plot of cell viability from figure 3(c), as a function of fluorescent intensity of $ONOO^-$ from figure 6(a), is shown in figure 7(a), where it is found that cell viability has a positive correlation with the fluorescent intensity of $ONOO^-$ produced by APPJs. At the low fluorescent intensity of $ONOO^-$, the cell viability is much higher, but at the high fluorescent intensity, the cell viability decreases sharply and almost reaches zero. Additionally, to obtain the concentration value of $ONOO^-$, the different concentrations of ONOONa are added to the medium and then are detected by a fluorescent probe with

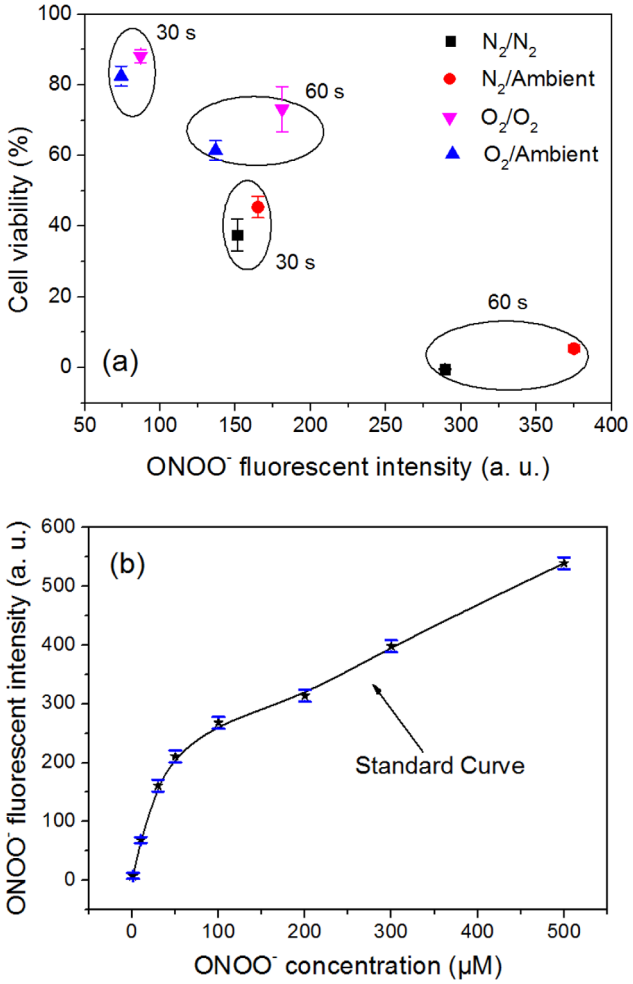

Figure 7. (a) A scatter plot of cell viability as a function of fluorescent intensity of $ONOO^-$, (b) a standard curve between the fluorescent intensity of ONOONa and the known concentrations of $ONOO^-$.

CBA. A standard curve between the fluorescent intensity of ONOONa and the known concentrations of $ONOO^-$ is also made in figure 7(b); it can be seen that the fluorescent intensity of $ONOO^-$ first sharply increases before 50 μM $ONOO^-$ and then shows an almost linear relationship with increase of concentrations of $ONOO^-$. The experiment results from figure 7 intuitively and clearly indicate that the cell viability has a positive correlation with the concentration of $ONOO^-$ generated by the APPJs treatment and the formation of $ONOO^-$ in the medium generated by APPJs plays an important role in the myeloma cell inactivation.

4. Results discussion

In our experiment, the pH value of the medium after APPJ treatment has remained at about 7.2. According to [2, 13, 32, 33], it is demonstrated that acidification alone does not induce comparable cell efficay independent on the plasma treatment; the pH is only to increase the reactivity of the radicals and itself has no direct effect on the cell inactivation. So the synergistic of pH and reactive species inducing cell death can be ignored in this study. In figure 2(a), the NO produced by N_2/N_2 and N_2/Ambient APPJs is considered to play a crucial role in cell death, and can react with water vapor and water in the medium, then transition to HNO_2 and HNO_3 into medium [2]. In figure 2(b), it seems that the O_2 APPJ with the O_2 shielding gas does not create RNS in the medium, but $ONOO^-$ can be formed in figure 6(a), which means that nitrogen oxides actually exist in the medium. The speculation is in good agreement with those published by Jablonowski *et al* [34] who used Ar as the feeding gas and used O_2 as the shielding gas, where about 600 nM NO_2^- and 200 nM NO_3^- can be measured in the medium. Reuter *et al* confirms that Ar APPJ treatment with pure N_2 shielding gas would lead to more HacaTs cell death than that of Ar APPJ treatment with a pure O_2 shielding gas. When the 20% O_2 and 80% N_2 as shielding gas, the death rate would reach the maximum value [28].

In the medium, the $ONOO^-$ is mainly generated by the following reactions [11, 35, 36].

$$e + N_2 \rightarrow 2N + e \quad (1)$$

$$N + O + N_2 \rightarrow NO + N_2 \quad (2)$$

$$NO + O_2^- \rightarrow ONOO^- \quad (3)$$

$$OH + HNO_2 \rightarrow NO_2 + H_2O \quad (4)$$

$$OH + NO_2 \rightarrow ONOOH. \quad (5)$$

According to the above reactions, it is found that the OH and O_2^- would react with NO or NO_2 to generate $ONOO^-$ by different pathways, which is the reason the production of O_2^- and OH may be low in N_2/N_2 APPJ, because they are so reactive with other components (such as NO and NO_2) in the medium, so the radical trappers do not have a chance to trap, while there is lots of production of OH and O_2^- in O_2/O_2 APPJ, which may be due to the fact that there are not enough NO and NO_2 to consume OH and O_2^- (figures 6(c) and (d)). As with the similar expression in the literature published by Lu *et al* [37] and Girard *et al* [18], the concentration of NO_2^- and NO_3^- in the medium drops drastically to a low level in the presence of the shielding gas of pure O_2.

It is sure that O_2^- and OH are both extremely reactive, but the O_2^- and OH may be of low concentrations and a short lifetime so they are not able to play the role of inducing cell death, because high concentration O_2^- and OH produced by O_2/O_2 APPJ in figure 6 would not result in a greater cell death rate, so it is reasonably considered that both O_2^- and OH are playing an important role in generating $ONOO^-$. A similar description can also been found in the literature published by Kushner *et al* who propose that $ONOO^-$ has a high oxidizing potential and is produced through OH reacting with NO_2, and O_2^- reacting with NO. Meanwhile, the reaction between O_2^- and NO nearly doubles the production of NO_3^- and $ONOO^-$ [12]. Additionally, in figure 6, some discussion about the temperature effects and plasma density should also be paid attention, because compared to the gas without shielding, the shielding gas flow would cause cooling for the medium, and the N_2 plasma jet is denser and thus produces more reactive species than that of the O_2 plasma jet.

It is commonly considered that the biologically-efficient RNS are $ONOO^-$ and NO_2^-, which would induce nitration and nitrosation of proteins and nucleic acids [16]. Especially, $ONOO^-$ is of major interest since its half-lifetime at pH 7.4 is about 1 s [38]. The $ONOO^-$ is toxic to the cell because of its ability diffuse in the medium and react with the cell walls to break biological structures and access the inside cell. Meanwhile, the $ONOO^-$ inside cell can also damage amino acids and nucleic acids, which would disrupt the function of the organelle [16]. Therefore, it is reasonably concluded that the formation of $ONOO^-$ in the medium generated by APPJ plays an important role in the cell inactivation [18, 39]. As reported in the literature published by Szabo *et al* [40] who used the He plasma treatment to produce $ONOO^-$ in the PBS(Ca^{2+}/Mg^{2+}), they think that the $ONOO^-$ would induce both cellular apoptosis and necrosis depending on the production rates, endogenous antioxidant levels and exposure time, and therefore could contribute to the plasma-induced cell death. Additionally, Lukes *et al* [2] recently reported that the formation of $ONOO^-$ plays an important role in the antibacterial activity.

However, there are many other factors (such as radicals, exited species, UV radiation, etc) that also may lead to cell apoptosis. For example, both Girard *et al* [18] and Mohades *et al* [41] suggest that the efficiency of plasma treatment strongly depends on the combination of H_2O_2 and NO_2^-, because the NO_2^- acts in synergy with H_2O_2 to enhance the cell death in normal and tumour cell lines. Additionally, they point to H_2O_2 as a central player in plasma-induced oxidative stress, where the concomitant production of NO_2^- exacerbates the H_2O_2 toxicity. In addition, one possible explanation about inducing cell death is the proximity of the APPJs to the medium for N_2/N_2 and O_2/O_2. Even if it is not a direct-contact/etching effect, the reactive species generated by N_2/N_2 APPJ is closer to the medium.

5. Conclusion

Atmospheric pressure N_2/N_2 and O_2/O_2 APPJs excited by a nanosecond pulse are generated. The corresponding simplex RNS and ROS are respectively delivered directly into the medium for the purpose of inducing myeloma cell apoptosis. The results show that the cell death rate by N_2/N_2 APPJ is more than two times that of the O_2/O_2 APPJ with a shielding gas. By measuring the reactive species of $ONOO^-$, H_2O_2, OH and O_2^- in the medium, it is found that the concentration of $ONOO^-$ after N_2/N_2 APPJ treatment is about two timesthat after O_2/O_2 APPJ treatment. Meanwhile, it confirms that cell viability has a positive correlation with the concentration of $ONOO^-$. Therefore, we propose that the formation of $ONOO^-$ in the medium generated by APPJs plays an important role in the myeloma cell inactivation.

Acknowledgments

This work was supported by the National Natural Science Foundation of China (Grant Nos. 51307135 and 51521065), and the State Key Laboratory of Electrical Insulation and Power Equipment (Grant Nos. EIPE17309 and EIPE14123).

References

[1] Graves D B 2014 *Plasma Process. Polym.* **11** 1120–7
[2] Lukes P, Dolezalova E, Sisrova I and Clupek M 2014 *Plasma Sources Sci. Technol.* **23** 015019
[3] Traylor M J, Pavlovich M J, Karim S, Hait P, Sakiyama Y, Clark D S and Graves D B 2011 *J. Phys. D: Appl. Phys.* **44** 472001
[4] Kong M G, Kroesen G, Morfill G, Nosenko T, Shimizu T, Van Dijk J and Zimmermann J L 2009 *New J. Phys.* **11** 115012
[5] Graves D B 2014 *Phys. Plasmas* **21** 080901
[6] Zhong S Y, Dong Y Y, Liu D X, Xu D H, Xiao S X, Chen H L and Kong M G 2016 *Br. J. Dermatol.* **174** 542
[7] Oh J S, Szili E J, Gaur N, Hong S H, Furuta H, Kurita H, Mizuno A, Hatta A and Short R D 2016 *J. Phys. D: Appl. Phys.* **49** 304005
[8] Kang W S, Hur M and Song Y H 2015 *Appl. Phys. Lett.* **107** 094101
[9] Oehmigen K, Hahnel M, Brandenburg R, Wilke C, Weltmann K D and Woedtke T V 2010 *Plasma Process. Polym.* **7** 250–7
[10] Bartis E A J, Knoll A J, Luan P, Seog J and Oehrlein G S 2016 *Plasma Chem. Plasma Process.* **36** 121–49
[11] Liu D X, Liu Z C, Chen C, Yang A J, Li D, Rong M Z, Chen H L and Kong M G 2016 *Sci. Rep.* **6** 23737
[12] Tian W and Kushner M J 2014 *J. Phys. D: Appl. Phys.* **47** 165201
[13] Marshall S E, Jenkins A T A and Al-Bataineh S A 2013 *J. Phys. D: Appl. Phys.* **46** 18540
[14] Szili E J, Oh J S and Hong S H 2015 *J. Phys. D: Appl. Phys.* **48** 202001
[15] Baek E J, Joh H M, Kim S J and Chung T 2016 *Phys. Plasmas* **23** 073515
[16] Girard F, Badets V, Blanc S, Gazeli K, Marlin L, Authier L, Svarnas P, Sojic N, Clément F and Arbault S 2016 *RSC Adv.* **6** 78457–67
[17] Tresp H, Hammer M U, Weltmann K D and Reuter S 2013 *Plasma Med.* **3** 45–55
[18] Girard P M, Arbabian A, Fleury M, Bauville G, Puech V, Dutreix M and Sousa J S 2016 *Sci. Rep.* **6** 29098
[19] Xiao D, Cheng C, Shen J, Lan Y, Xie H, Shu X, Meng Y, Li J and Chu P K 2014 *Phys. Plasmas* **21** 053510
[20] Tang J, Jiang W, Li J, Wang Y, Zhao W and Duan Y 2015 *Appl. Phys. Lett.* **107** 083505
[21] Zhang C, Shao T, Zhou Y, Fang Z, Yan P and Yang W 2014 *Appl. Phys. Lett.* **105** 044102
[22] Xu D H, Luo X H and Xu Y J 2016 *Biochem. Biophys. Res. Commun.* **473** 1125–32
[23] Zielonka J, Zielonka M, Sikora A, Adamus J, Joseph J, Hardy M, Ouari O, Dranka B P and Kalyanaraman B 2012 *J. Biol. Chem.* **287** 2984–95
[24] Wu H Y, Sun P, Feng H Q, Zhou H X, Wang R X, Liang Y D, Lu J F, Zhu W D, Zhang J and Fang J 2012 *Plasma Process. Polym.* **9** 417–24
[25] Tresp H, Hammer M U, Winter J, Weltmann K D and Reuter S 2013 *J. Phys. D: Appl. Phys.* **46** 435401
[26] Shao T, Long K, Zhang C, Yan P, Zhang S and Pan R 2008 *J. Phys. D: Appl. Phys.* **41** 215203
[27] Yang D Z, Wang W C, Zhang S, Tang K, Liu Z J and Wang S 2013 *Appl. Phys. Lett.* **102** 194102
[28] Reuter S, Winter J, Ansgar S B, Tresp H, Hammer M U and Weltmann K D 2012 *IEEE Trans. Plasma Sci.* **40** 2788–94
[29] Yang D Z, Yang Y, Li S Z, Nie D X, Zhang S and Wang W C 2012 *Plasma Sources Sci. Technol.* **21** 035004

[30] Iseni S, Bruggeman P J, Weltmann K D and Reuter S 2016 *Appl. Phys. Lett.* **108** 184101
[31] Xu D H, Wang B Q, Xu Y J, Chen Z Y, Cui Q J, Yang Y J, Chen H L and Kong M G 2016 *Sci. Rep.* **6** 27872
[32] Machala Z, Tarabova B, Hensel K, Spetlikova E, Sikurova L and Lukes P 2013 *Plasma Process. Polym.* **10** 649–59
[33] Ikawa S, Kitano K and Hamaguchi S 2010 *Plasma Process. Polym.* **7** 33–42
[34] Jablonowski H, Hansch M C, Dunnbier M, Wende K, Hammer M U, Weltman K D, Reuter S and Woedtke T 2015 *Biointerphases* **10** 029506
[35] Chen C, Liu D X and Liu Z C 2014 *Plasma Chem. Plasma Process.* **34** 403–11
[36] Liu Z C, Liu D X, Chen C, Li D, Yang A J, Rong M Z, Chen H L and Kong M G 2015 *J. Phys. D: Appl. Phys.* **48** 495201
[37] Lu X, Naidis G V and Laroussi M 2014 *Phys. Rep.* **540** 123–66
[38] Pfeiffer S, Gorren A C, Schmidt K, Werner E R, Hansert B, Bohle D S and Mayer B 1997 *J. Biol. Chem.* **272** 3465–70
[39] Daiber A, Daub S, Bachschmid M, Schildknecht S, Oelze M, Steven S, Schmidt P, Megner A, Wada M and Tanabe T 2013 *Int. J. Mol. Sci.* **14** 7542
[40] Szabo C, Ischiropoulos H and Radi R 2007 *Nat. Rev. Drug. Discov.* **6** 662–80
[41] Mohades S, Laroussi M, Sears J, Barekzi N and Razavi H 2015 *Phys. Plasmas.* **22** 122001